Mechanical Characterization of a Multi-Stage Passive Compliant End-Effector for Aerial NDT

Luka Greblo, Marko Car, Antun Ivanović, Jurica Goričanec, Lovro Marković, Matko Orsag, Stjepan Bogdan

***Abstract*— This paper presents the design and mechanical characterization of a multi-stage passive compliant end-effector designed to enable stable physical interaction on curved and planar marine surfaces. The proposed tool utilizes a dual-layer compliance strategy: a linear spring system for axial impact damping and a polyurethane flexure for multi-axis angular alignment. We employ Finite Element Method (FEM) analysis to validate the structural integrity of the polyurethane joint, focusing on axial and shear strain distributions to ensure high safety margins against material failure. Experimental results, validated via a high-precision motion capture system, demonstrate the tool's ability to passively compensate for up to 15 degrees of surface misalignment. This "hardware-first" approach reduces the burden on flight control systems, providing a robust pathway for standard UAVs to perform contact-based inspection.**

I. INTRODUCTION

In the context of maritime and offshore infrastructure, visual inspection is now a routine industrial service; however, contact-based Non-Destructive Testing (NDT)-such as ultrasonic thickness gauging-has yet to see widespread adoption [1], [2]. The primary barrier to industrialization is the lack of autonomous solutions that can be retrofitted onto existing, standard underactuated fleets.

Currently, the industry relies on stock multirotors optimized for flight endurance and payload capacity. These platforms are inherently underactuated, making the maintenance of stable contact forces on vertical ship hulls or curved offshore pillars a significant mechanical and control challenge [3], [4]. While specialized fully-actuated or omnidirectional platforms have been developed in academic settings to handle multi-axis forces [5], [6], their high cost, mechanical complexity, and reduced flight times prevent them from being integrated into standard industrial inspection workflows.

Consequently, there is a clear demand for "plug-and-play" hardware that enables existing underactuated UAVs to perform physical probing without requiring a total overhaul of the platform's architecture. Most research to date has focused on complex, high-bandwidth control loops to manage the contact transient [7], [8]. However, these software-heavy approaches often require modifications of the airframe and unpredictable dynamics of real-world environments, such as wind gusts and surface biofouling.

In this work, we propose that the bridge between scientific research and industrial application lies in passive mechanical intelligence. We present a multi-stage compliant end-effector designed specifically to be retrofitted onto standard underactuated UAVs. By moving the complexity of surface alignment and impact absorption from the flight controller to a passive mechanical tool, we enable stable NDT on marine-representative surfaces. This study focuses on the structural characterization of this tool through Finite Element Method (FEM) analysis and high-precision validation in a motion capture environment, providing a pathway for standard fleets to transition from visual-only to contact-capable platforms.

Authors are with Faculty of Electrical and Computer Engineering, University of Zagreb, 10000 Zagreb, Croatia (luka.greblo, marko.car, antun.ivanovic, jurica.goricanec, lovro.markovic, matko.orsag, stjepan.bogdan) at fer.hr

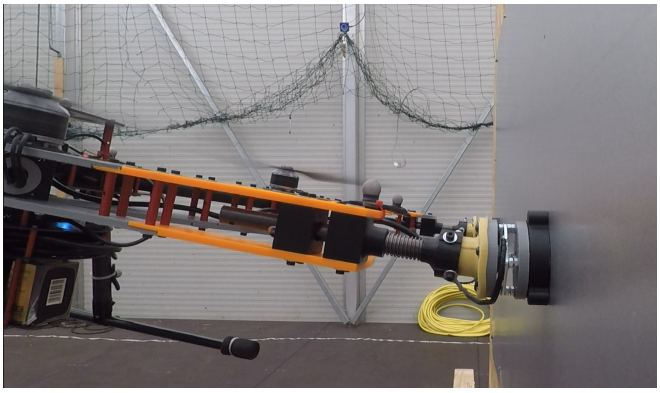

Fig. 1: Passive end effector in contact with metallic surface for NDT.

II. SYSTEM OVERVIEW

This section details the hardware architecture of the compliant end-effector, specifically designed to bridge the gap between visual inspection and contact-based NDT for standard underactuated UAVs. The design philosophy centers on passivity of mechanical multi-stage compliance to absorb impact transients and self-align to surfaces, thereby reducing the dependency on high-bandwidth flight control.

A. Design Requirements and Constraints

The design is governed by two primary industrial constraints. First, to maintain compatibility with existing commercial multirotors, the system must remain lightweight and avoid complex multi-axis active DoF manipulators. Second, sensing is intentionally restricted to a single-axis load cell to minimize payload weight.

Because standard X-frame UAVs are underactuated, any attempt to regulate contact force via pitching inherently introduces lateral coupling. In a rigid system, this coupling leads to "roll-sliding," where small orientation errors result in the end-effector drifting across the inspection surface. Rather than solving this exclusively through complex control

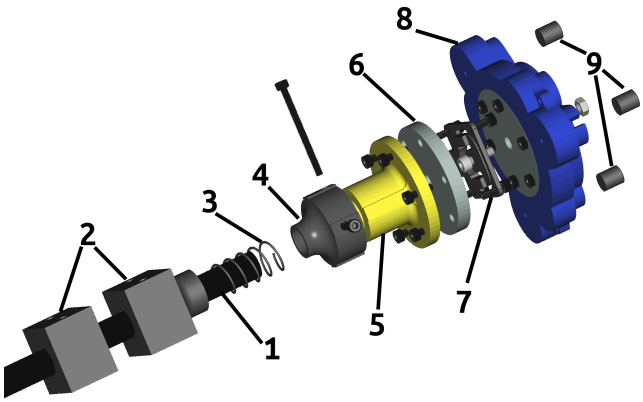

Fig. 2: Exploded tool blueprint

laws, this approach utilizes a multi-stage passive compliance system to mechanically decouple these dynamics.

B. Multi-Stage Compliant End-Effector

The end-effector 1 manages the fast dynamics of the contact transient where the ”first touch” of 7 kg mass of the UAV meets the rigid environment. The mechanism consists of three functional stages first of which is axial damping stage consisting of a parallel pair of linear springs with a combined stiffness of 225 N/m to match parameters of impedance controller and a 35 mm stroke. This stage acts as a mechanical low-pass filter, cushioning the initial impact and storing energy to prevent the UAV from rebounding off the surface before the impedance controller can respond. Second is angular alignment stage. A flexible polyurethane (PU) flexure joint. This component is critical for maritime applications involving curved hulls or non-orthogonal approach angles. The Shore 65 compound was selected following iterative testing; softer compounds exhibited parasitic oscillations during flight, while stiffer materials failed to provide sufficient pitch compensation under the torques generated by the UAV's contact pose. The distal end houses a single-axis load cell and a magnetic assembly with a 3 N pull force. This ensures stable attachment to ferrous surfaces, such as ship hulls, allowing the NDT sensor to maintain the ”firm pressure” required for accurate porosity or thickness measurements.

C. Structural Breakdown

The hardware assembly is optimized for low mass (around 150g each side) and high axial fidelity 2:

- Linear Guidance: A carbon fiber shaft (1) slides within low-friction guide blocks (2), ensuring that contact forces are directed strictly along the sensor's measurement axis.
- Compliance Path: The compression spring (3) and the PU joint (5) are serialized to provide both 1D translation and 3D angular yielding.
- Sensor Integration: A single-axis Kern CK 30-Y1 load cell (7) is positioned behind the contact tip. By placing the sensor after the primary compliance stages, we isolate it from high-frequency impact shocks that could saturate or damage the strain gauges.
- NDT Interface: The blue distal module (8) is a modular holder designed for porosity sensors, allowing the tool to be adapted for different NDT modalities.

D. Structural Validation via FEM

To ensure the reliability of the PU flexure, we employ Finite Element Method (FEM) analysis. For elastomers, failure is characterized by tearing (rupture) rather than brittle snapping. Equivalent Plastic Strain and YY-directional Strain were analyzed to define operational limits.

The polyurethane (PU) flexure is modeled as a passive, multi-axis revolute joint that provides the necessary degrees of freedom (DoF) to decouple the UAV's attitude from the end-effector's contact orientation. By mapping the angular deflection limits in the FEM environment, we characterized the tool's ”passive workspace” to be the range within which the tool can maintain a flush surface-normal interface without active compensation from the flight controller.

The simulation results indicate that the joint can passively compensate for a misalignment of up to 15 degrees. Beyond this threshold, the increased force required to maintain engagement induces an excessive pitching angle, potentially compromising the stability and safety of the UAV. This capacity is critical for two reasons. First, underactuated multirotors must pitch forward to generate the longitudinal force required for NDT probing. Second, the PU joint absorbs this pitching motion, preventing the contact tip from prying away from the surface. When transitioning from planar ship hulls to curved geometries (such as pillars, pipes, or curved tank internals), the joint yields to the local surface normal.

Symmetry and Load Distribution due to the radial symmetry of the flexure joint and the distal hard plastic plate, the mechanical response is invariant to the direction of the bending moment. Consequently, the load required to accommodate a 15 degrees UAV pitch angle on a flat wall is analytically equivalent to the load required to inspect a curved surface with a corresponding tangential slope. This geometric compatibility ensures that the UAV can transition between varying geometries, as the passive hardware handles the local kinematic constraints.

E. Numerical Results and Discussion

The structural response of the multi-stage end-effector was evaluated by analyzing the normal strain components during a simulated contact event. As established in the design requirements, the polyurethane (PU) flexure must provide sufficient axial compliance to protect the rigid ABS interface and the UAV frame.

The axial strain distribution, ϵ_{yy}, is visualized for both the external surface in 3a and the internal cross-section in 3b. The results show a maximum compressive strain localized at the core of the flexure joint.

The peak strain recorded in the simulation reaches approximately 0.106, which corresponds to a 10.5% deformation. Given that industrial-grade polyurethane of Shore 65A hardness exhibits an elongation at break significantly exceeding 300%, the proposed design maintains a safety factor of over

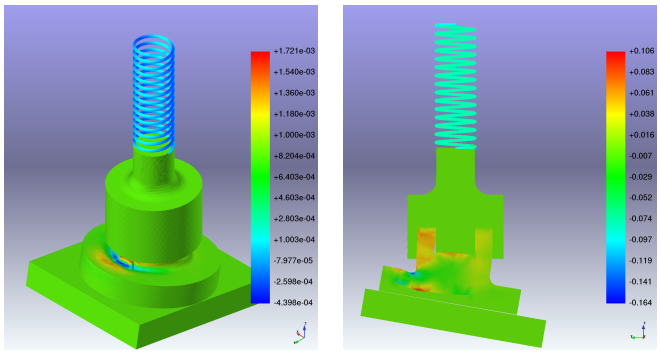

(a) External surface strain (b) Internal cross-section strain

Fig. 3: FEM visualization of axial normal strain (ϵ_{yy}) under peak operational load. The dimensionless scale represents mm/mm deformation.

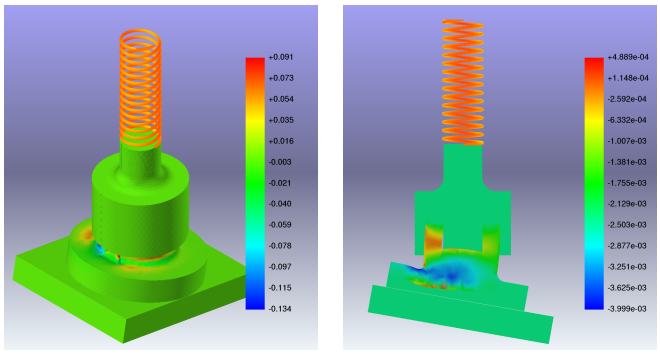

(a) External surface strain (b) Internal cross-section strain

Fig. 4: FEM visualization of axial normal strain (ϵ_{xx}) under peak operational load. The dimensionless scale represents mm/mm deformation.

60 against tearing or "ripping." This high margin of safety ensures that the tool can undergo thousands of contact cycles without material fatigue.

III. Experimental Validation in Motion Capture Environment

Experimental validation was conducted using a motion capture system to provide pose estimation of the UAV. The objective was to evaluate autonomous contact inspection, force regulation, and repeatability of the impedance controller.

The core of the autonomous approach relies on real-time environmental awareness via an onboard 3D LiDAR. To identify the inspection target within a cluttered point cloud, the system employs a Random Sample Consensus (RANSAC) algorithm. As illustrated in the provided scan data 7. The RANSAC algorithm processes the raw point cloud to effectively isolate the target surface from the surrounding environment and the contact target plane, representing the extracted planar inliers as the white points seen in the visualization. Once the plane is localized, the system automatically computes a surface normal vector, represented by the red arrow, which serves as the primary orientation reference for the flight controller. This normal vector is essential for defining the precise approach trajectory, ensuring

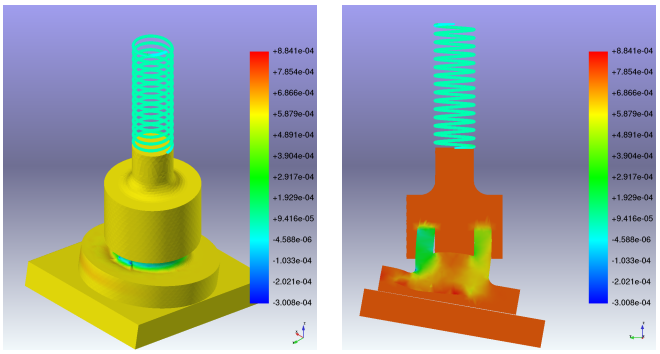

(a) External surface strain (b) Internal cross-section strain

Fig. 5: FEM visualization of axial normal strain (ϵ_{zz}) under peak operational load. The dimensionless scale represents mm/mm deformation.

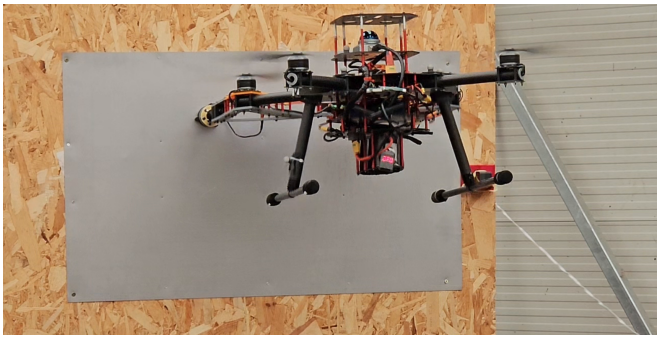

Fig. 6: UAV in contact with metallic plane.

the UAV aligns its end-effector perpendicularly to the surface to facilitate stable contact and accurate force regulation. Additionally, the small red cluster positioned at a distance from the plane denotes the UAV's current position, providing a clear spatial relationship between the sensor origin and the identified inspection target. A critical safety feature of this workflow is the pilot-in-the-loop verification. While the plane detection is fully automated, the UAV remains in a position holding mode until the pilot reviews the geometric fit. Once the operator acknowledges that the detected plane and normal vector accurately represent the physical target, the autonomous sequence is triggered. The FSM handled initialization, surface alignment, approach, contact establishment, measurement execution, and safe detachment. After entering autonomous mode, the system first performed sensor bias estimation and perception initialization. The detected surface normal was used to align the task frame, after which the UAV

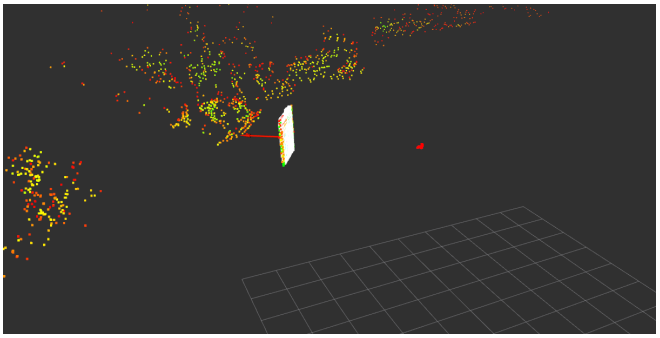

Fig. 7: LiDAR scan of the planar contact surface.

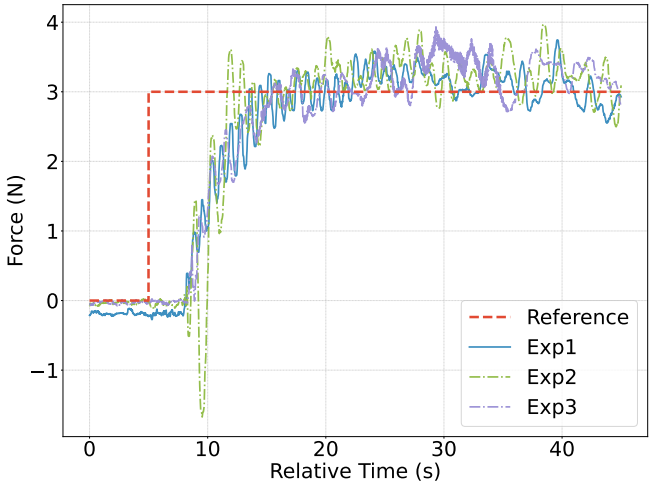

Fig. 8: Contact forces over several experiments

autonomously approached the target contact pose. Contact was detected using the load cell threshold, triggering the measurement phase with impedance-based force regulation. After the measurement interval elapsed, the UAV performed a controlled retreat and returned to a safe hover state. This state-machine structure ensured deterministic execution and allowed repeated trials under identical conditions. Safety monitoring ran in parallel, supervising force limits and state transitions, with immediate fallback to manual control in case of violations.

Multiple autonomous trials were performed within the motion capture workspace as it can be seen in the 6. The UAV consistently aligned with the detected surface, established contact, regulated the desired normal force, and detached after completing the inspection sequence. The ground-truth motion capture data confirmed stable approach trajectories, minimal lateral drift, and repeatable contact behavior across runs. Minor deviations were observed only during the initial impact phase due to mechanical compliance and estimator noise, after which steady-state force tracking remained consistent. In order to maintain stable contact, the adaptation law proposed in [9] was implemented. The adaptation parameter corresponds to the estimated environmental stiffness, allowing the controller to regulate interaction forces and establish stable contact with metallic surfaces of varying compliance. The quantitative performance of the system is best captured in the contact force profiles shown in Figure 8. The plots demonstrate repeatability across multiple autonomous trials, with force trajectories following a nearly identical evolution in each run. During the initial impact phase, the impedance controller successfully manages kinetic energy transfer, limiting force overshoots to a narrow range despite the high stiffness of the metallic target. Once contact is established, the adaptation law effectively compensates for environmental stiffness, leading to a highly stable steady-state phase where the desired force is maintained. The high degree of overlap between the individual trial curves confirms that the system can reliably replicate inspection forces without manual tuning or operator intervention. Furthermore, the steady force profiles during the measurement interval indicate a stable interaction, supporting consistent contact between the UAV and the surface for the duration of the inspection.

IV. CONCLUSION

This work presents the design and structural characterization of a passive compliant end-effector tailored for aerial NDT. By shifting the complexity of surface alignment and impact absorption from the flight controller to the mechanical hardware, we enable standard underactuated UAVs to maintain stable contact on complex geometries.

Our FEM analysis confirms that the polyurethane flexure joint operates well within its elastic regime, providing a ”mechanical fuse” effect that protects both the onboard sensors and the aircraft frame from impulsive contact loads. Specifically, strain visualizations demonstrate that the tool can accommodate significant pitching and curvature-induced misalignments (up to 15 degrees) without reaching material rupture thresholds. High-precision validation through motion capture system feedback experiments further confirms that this passive intelligence successfully decouples the UAV’s attitude from the contact interface. Future work will focus on integrating specialized NDT probes into the modular distal mount to evaluate long-term material fatigue during extended deployment.

ACKNOWLEDGMENT

This work was supported in part by the project ”Contact based inspection of transition piece by unmanned aerial vehicles” funded by the European Union - NextGeneration EU under Grant NPOO.C3.2.R2-I1.05.0018

REFERENCES

[1] T. E. Kon, “The importance of the use of unmanned aerial vehicles (uavs) in the oil and gas industry,” *Petroleum Science and Engineering*, vol. 8, no. 2, pp. 63–69, 2024.

[2] F. L. P. et al., “An uav system for visual inspection and wall thickness measurement in ships’ cargo tanks,” *Maritime Inspection Journal*, 2024.

[3] A. Ollero, M. Tognon, A. Suarez, D. Lee, and A. Franchi, “Past, present, and future of aerial robotic manipulators,” *IEEE Transactions on Robotics*, vol. 37, no. 5, pp. 1340–1356, 2021.

[4] V. Lippiello, J. Cacace, and A. Santamaria, “Novel aerial manipulator for accurate and robust industrial ndt,” *Sensors*, vol. 19, no. 6, p. 1305, 2019.

[5] A. Keipour, M. Mousaei, A. T. Ashley, and S. Scherer, “Integration of fully-actuated multirotors into real-world applications,” in *2018 IEEE International Conference on Robotics and Automation (ICRA)*, 2018, pp. 1–5.

[6] K. Bodie, M. Brunner, M. Pantic, S. Walser, P. Pfandler, U. Angst, R. Siegwart, and J. Nieto, “An omnidirectional aerial manipulation platform for contact-based inspection,” in *Robotics: Science and Systems*, Freiburg im Breisgau, Germany, June 22–26 2019.

[7] G. Nava, Q. Sablé, M. Tognon, D. Pucci, and A. Franchi, “Direct force feedback control and online multi-task optimization for aerial manipulators,” *IEEE Robotics and Automation Letters*, vol. 5, no. 2, pp. 331–338, 2020.

[8] M. Tognon, H. A. T. Chávez, E. Gasparin, Q. Sablé, D. Bicego, A. Mallet, M. Lany, G. Santi, B. Revaz, J. Cortés, and A. Franchi, “A truly-redundant aerial manipulator system with application to push-and-slide inspection in industrial plants,” *IEEE Robotics and Automation Letters*, vol. 4, no. 2, pp. 1846–1851, 2019.

[9] M. Car, “Control system for an unmanned aerial manipulator interacting with the environment based on a generalized model,” Ph.D. dissertation, University of Zagreb, Faculty of Electrical Engineering and Computing, 2023. [Online]. Available: https://urn.nsk.hr/urn:nbn:hr:168:919807